COMMUNICATION

Check for updates

Emerging environmental contaminants at the air/aqueous and biological soft interfaces†

Giada Dalla Pozza, Danielle Deardorff and Mahamud Subir [ID] *

Detection of micropollutants, such as pharmaceuticals and industrial chemicals with endocrine disrupting potency, in ground and surface waters is of emerging concern. Within the aquatic environment, these emerging contaminants (ECs) can interact with various surfaces and biological membranes. The implication is that, provided the ECs exhibit sufficient affinity, these surfaces can modulate their fate and transport properties. Knowledge of the types of interactions with biomembranes can also help decipher their impact on aquatic organisms. Here, we show that selected organic micropollutants – amlodipine (AMP), carbamazepine (CBZ), β-estradiol (β-ED), and 4-propylphenol (4-PP) – exhibit proclivity for the air/aqueous interface. These compounds also interact differently with a zwitterionic phospholipid membrane. The adsorption free energy for the water surface, in the order of increasing affinity, is as follows: 4-PP < AMP < β-ED ∼ CBZ. Of the four compounds studied, 4-PP has the greatest extent of disruption of the phospholipid membrane. Our results suggest that the extent of interaction with the water surface and biological membrane is dependent upon the chemical nature of these micropollutants. This fundamental study highlights the importance of interfacial chemistry on the fate and transport of emerging contaminants in natural waters.

Introduction

Understanding chemical interactions of emerging contaminants (ECs) is vital to the knowledge of their fate and transport within the aquatic environment. Aqueous phase photolysis, biodegradation, and sorption into the soil phase are often considered as primary fate and transport pathways of ECs in the aquatic ecosystem.[1–3] However, there are numerous soft interfaces with which aquatic pollutants can interact. These include the water surface, polymeric substrates of particulate matters (*e.g.*, microplastics and colloidal organic matter), and biological membranes of aquatic organisms. Once adsorbed, these

Department of Chemistry, Ball State University, USA. E-mail: msubir@bsu.edu

† Electronic supplementary information (ESI) available. See https://doi.org/10.1039/d2va00081d

Environmental significance

The ubiquity of pharmaceuticals and personal care products (PPCPs) in the aquatic environment is of emerging societal concern. Key pathways of fate and transport can include adsorption onto various surfaces (*e.g.*, air/aqueous interface) and interaction with aquatic organisms. Therefore, understanding their proclivity for air/aqueous interfaces and impact on biological membranes is essential. Investigations pertinent to the adsorption of emerging contaminants (ECs) at soft interfaces are lacking. The key finding of this communication is that PPCPs can and do adsorb at the air/aqueous interface. The extent of their interaction with biological membranes depends on the type of contaminant. The implication is that surface interactions of ECs need to be considered to fully address their impact on the environment.

organic compounds are not only removed from the aqueous phase but are also susceptible to exhibiting altered photochemical reactivity. Interfacial adsorption can lead to orientational restriction, spectral shift, and thus, a change in the efficiency of photon uptake in these molecules.[4–6] This can result in altered photokinetic pathways. For example, a distinct photolysis rate, as compared to that of aqueous phase photochemistry, has been reported for molecules adsorbed at the surface of microplastics and in the presence of natural organic matter.[4,7–11] From the point of view of wastewater treatment, understanding the fundamentals of EC–surface interaction is also essential for developing remediation techniques for removing emerging contaminants based on adsorption technology.[12–14] Knowledge of the type of interactions (hydrophobic, H-bonding, *etc.*) can guide the development of better sorbents.

In addition to the colloidal interfaces there are planar interfaces with which micropollutants can interact. For instance, about two-thirds of the planet earth is an air/aqueous interface. Adsorption is the first step for surface mediated photochemistry. Thus, understanding the proclivity of micropollutants for the water surface is warranted. Similarly, organic pollutants can interact with aquatic organisms and disrupt their biological membranes.[15,16] Many pharmaceuticals (including human and veterinary medicine) are designed to

permeate across lipid membranes and thus can have adverse effects on microorganisms and aquatic animals. For example, endocrine disrupting chemicals (EDCs) such as β-estradiol (β-ED or E2), can cause reproduction toxicity in fish and frogs.[17,18] Bioaccumulation of carbamazepine (CBZ), a most frequently detected active pharmaceutical ingredient, by algae has been reported.[19,20] Biological cells and organelles are composed of phospholipids. Thus, how these compounds and their metabolites interact at the biointerface of lipid membranes is critical to decipher the toxic effect of these drug contaminants.

In the recent decades, important field work on the detection of ECs and their impact on aquatic organisms has emerged.[21–25] Studies involving their occurrence and removal strategies exist.[26–28] Nevertheless, studies involving their interactions with various surfaces remain scarce. In this communication, we explore the affinities of selected micropollutants for the air/aqueous interface and their interaction with a zwitterionic phosphatidylcholine lipid membrane. Phospholipids are a dominant lipid class and are common in the cell membranes of aquatic organisms and marine environments.[29–32] To assess the adsorption of pharmaceutical contaminants, CBZ, β-ED, and amlodipine (AMP) have been selected for this study. These micropollutants are detected in various aquatic environments and are currently listed among the top priority emerging organic contaminants based on five different prioritization schemes.[33] On the other hand, 4-propylphenol (4-PP) represents one of many alkylphenols used in personal care products. Similar to β-ED, 4-PP also has endocrine disrupting capability.[34]

The ubiquity of these ECs in the aquatic environment is one of the main reasons for selecting them in this study. The concentrations of these compounds in the environment vary with the source of the water and show regional variations. For example, the average global maximum concentration of CBZ in groundwaters has been reported to be 5×10^3 ng L^{-1}.[35] In Portugal, hospital effluents showed a range of 45.5–195 ng L^{-1} of AMP.[36] For β-ED, a concentration range of 2.4–670 ng L^{-1} in wastewater has been reported.[37] Alkylphenols as high as 644 μg L^{-1} have been reported in Spanish rivers.[38,39] Along with the above discussion highlighting the significance of these contaminants, they are also representative of a wide variety of micropollutants in the aquatic environment. Moreover, these compounds exhibit distinct structural and chemical properties. For instance, the rotatable bond count (RBC) for both CBZ and β-ED is zero; whereas, AMP and 4-PP has an RBC of 10 and 2, respectively (HMDB and Drug Bank databases).[40,41] The implication is that CBZ and β-ED are rigid and AMP is flexible. Based on their pK_a values,[41–43] CBZ (15.96), β-ED (10.77), and 4-PP (10.31) exist dominantly as neutral species, and AMP (9.45, strongest basic) exhibits a positive charge in neutral water. Thus, elucidating the influence of their chemical properties on their interaction with bio-membranes and interfacial water is also of fundamental interest. Tantalizing results of EC–surface interactions and their impact on model bio-membranes, as assessed by surface tensiometry, are the subject of this communication.

The aim of this study thus can be summarized as follows: to (1) determine the air/aqueous surface proclivity of representative emerging organic contaminants, (2) elucidate their impact on model biological membranes, and (3) provide a preliminary assessment on the structure–functional relationship between the pollutant molecules and their interfacial behaviors. We have accomplished these objectives by experimental measurements of surface tension of the air/water interface and surface pressure of the lipid monolayer in the presence and absence of the target contaminants. By exploring the surface effect at various bulk concentrations of ECs, energetics of their interactions have been determined. Given that ECs are pervasive and that there is an abundance of surfaces in the aquatic environment, understanding the interfacial behavior of these contaminants is significant. The majority of existing research on environmental contaminants focuses on bulk or solution phase properties; thus, fundamental insights into their surface interaction is not only original but also necessary. The findings reported herein are unique and contribute to an overall understanding of ECs in the environment.

Materials and methods

Amlodipine (SKU PHR1185), carbamazepine (SKU 94496), β-estradiol (SKU E8875), 4-propylphenol (SKU P53802), and 1,2-dipalmitoyl-*sn*-glycero-3-phosphocholine (DPPC) (SKU P0763) were purchased from Sigma Aldrich and used as received. Aqueous solutions of the organic compounds were prepared using Milli-Q water (18.2 MΩ cm). DPPC was prepared in chloroform (99.8% ACS reagent grade, Sigma Aldrich) at a 0.5 mg mL^{-1} concentration. All glassware was cleaned with aqua regia (3 : 1 HCl/HNO$_3$). Stock solutions of the organic compounds were prepared slightly below their solubility limits and kept in the refrigerator until further dilutions were needed for the experiments. The solubilities of these compounds in Milli-Q water at 22 °C have been estimated in our lab experimentally. In the order of increasing solubility, they are 47 μM for β-ED, 75 μM for CBZ, 132 μM for AMP, and ∼8 mM for 4-PP. Fresh samples were prepared on a weekly basis.

Surface tension measurement at the air/aqueous interface

To determine the surface proclivity of the selected ECs, the method of surface tensiometry has been employed. A small Langmuir–Blodgett trough (LBT) apparatus (KN2001, KSV NIMA) was used to determine the surface tension, γ, at the air/water interface. Applying the Wilhelmy plate method,[39] surface tensions of different solutions containing the desired concentration of micropollutant were measured. Each solution (22 mL) was poured into a Teflon dish (3.1 cm inner diameter), and allowed to equilibrate for 20 minutes before surface tension was measured using the Wilhelmy plate. At least 3 measurements for each concentration were made. The surface tension (γ) *vs.* concentration (c) plots show the average of these independent measurements.

Surface pressure *vs.* area isotherm measurement

Measurement of surface pressure upon compressing insoluble lipids at the air/water interface was conducted using an LBT.

This apparatus senses the surface tension and as the area of the trough is reduced it generates a surface pressure *vs.* molecular area ($\pi-A$) isotherm. The isotherms were measured in the presence and absence of micropollutants in the subphase. The surface pressure (π) is defined as $\gamma_o - \gamma_1$, where γ_o is the surface tension of the clean interface and γ_1 is that of an interface with an insoluble monolayer.[44] A thorough cleaning and monolayer preparation protocol was performed prior to each experimental measurement. This includes, rinsing the Teflon components of the LBT balance with 200 Proof ethanol, followed by rinsing with abundant Milli-Q water, and drying the trough surfaces with UHP N_2 gas. The Wilhelmy plate was also rinsed with pure ethanol and Milli-Q water. Then, it was burned using a butane torch until red hot to remove any residual organic compounds. For the π *vs.* A measurements, the LBT Teflon base was filled with 57 mL of Milli-Q water (or aqueous solution of the target compound). Approximately one-half of the Wilhelmy plate was submerged in the solution at the centre of the well. Using a software, the balance was zeroed. The barriers were then compressed and the pressure was monitored. Prior to adding DPPC, it was ensured that the surface pressure upon compressing the neat water remained below 0.3 mN m^{-1}. This served as an indication that the neat water subphase remained free of surfactants and other impurities. If the surface pressure reading was slightly above tolerance, the surface water was cleaned by aspirating it with a siphon vacuum cleaner, followed by refilling the base with fresh water as needed. If a subtolerance value not achieved, the cleaning procedure was repeated.

To prepare the DPPC monolayer, using a micro syringe, 15 μL of DPPC/chloroform solution was distributed dropwise at different locations over the entire water surface. Then 15 minutes was allocated for the chloroform to evaporate. An additional 30 minutes was given for the subphase containing the target contaminants to reach an equilibrium with the phospholipid. During this waiting period and while the measurement was conducted, the LBT apparatus was covered with a shield in order to avoid contaminations from dusts and prevent disruptions from any airflow in the lab. The trough was temperature controlled @ 22 °C by flowing water from a chiller through the LBT baseplate. The insoluble film was compressed at an average rate of 0.083 cm^2 s^{-1}. Replicates of $\pi-A$ isotherms were recorded for each concentration of the micropollutant. Each data point in the isotherm represents an average value obtained from independent trials. The data analysis of both $\pi-A$ isotherms and surface tension measurements were conducted using IgorPro, Wavemetrics software.

Results and discussion

Adsorption onto the air/aqueous interface

The surface tension of neat water is reduced when organic molecules are adsorbed at the water surface. This principle has been the basis of determining the Gibbs surface excess, Γ. Fig. 1 shows the Γ *vs.* c plots for the compounds investigated in this study. The upper value of the bulk concentration for each micropollutant is restricted by its solubility limit in water. These
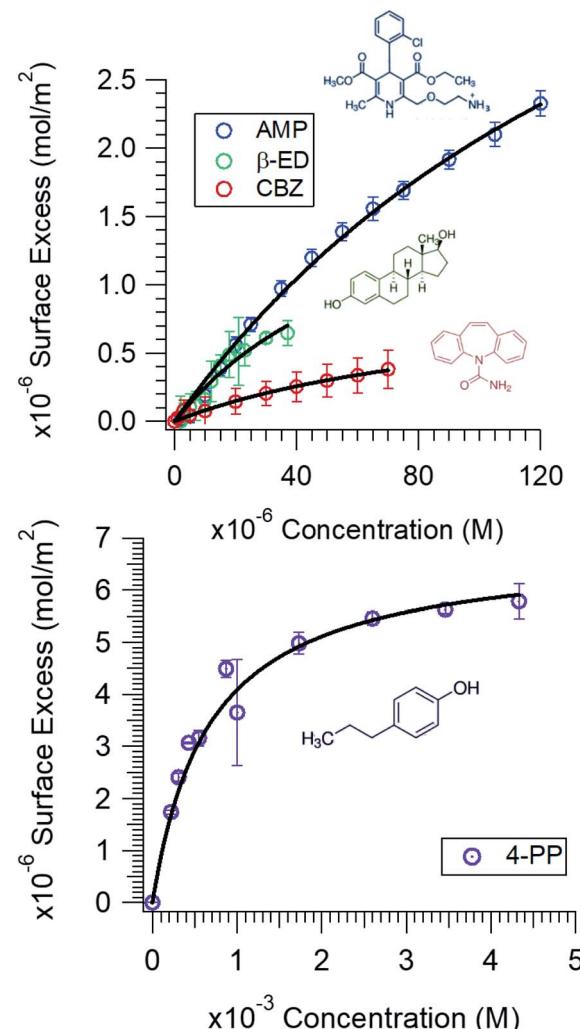

Fig. 1 Adsorption isotherms (surface excess *vs.* initial concentration) of AMP, β-ED, CBZ (Top) and 4-PP (Bottom) for the air/aqueous interface. The solid black traces correspond to the Langmuir fits of the experimental data. Images of molecular structures are from Sigma Aldrich.

isotherms allow the determination of the energetics of the adsorption process. However, at this juncture a description of how the Γ *vs.* c plot was generated is warranted.

In brief, the slope of the γ *vs.* c plot is related to Γ as follows:

$$\Gamma = -\frac{c}{RT}\frac{d\gamma}{dc} \qquad (1)$$

where R is the gas constant and T is the Kelvin temperature.[44,45] Thus, for each micropollutant, the surface tension data were plotted against its solution phase concentration (Fig. A1 in the ESI†). The decrease in γ observed with increasing concentration resembles the adsorption of amphiphiles at the air/aqueous interface. Plotting the concentration on a log-scale, it is apparent that at a low concentration there is a slow decrease in γ, followed by a sharp drop in surface tension at a higher concentration. This behaviour is best described using a 2nd or 3rd degree polynomial function.[46] This empirical fit allows the

simulation of the dependence of surface tension on concentration and the derivative of the continuous fit function is taken instead of the discrete data points. Each plot was thus fitted using a polynomial equation, from which the slope, $\frac{d\gamma}{dc}$, was determined. These plots and the fit parameters are shown in the ESI.† The value of Γ (in mol m^{-2}) at different concentrations was determined based on eqn (1).

It is clear (Fig. 1) that all these compounds show surface activity, but the extent of surface coverage varies. In Table 1, the area occupied per molecule at the highest concentration investigated is reported for each of these compounds. Given that the surface coverage values for both AMP and 4-PP are close to their molecular dimensions, it is apparent that these contaminants have reached full coverage at their respective concentrations. However, the surface coverage of CBZ and β-ED are not completely saturated. A possible reason is that these rigid and roughly leaflet-like compounds lie flat and thus occupy a greater area. The adsorption isotherms also show a Langmuirian behaviour. Thus, fitting the data using the Langmuir model (eqn (2)),[44,45] we have further obtained the equilibrium constant, K_{ads}, and maximum surface excess, Γ_{max}.

$$\Gamma = \Gamma_{max} \frac{K_{ads}\frac{c}{c_o}}{K_{ads}\frac{c}{c_o} + 1} \qquad (2)$$

In this equation, c_o represents the concentration of water, which is 55.5 M, and c corresponds to the equilibrium concentration of the target compound remaining in the solution. However, since the depletion of the solution phase species is negligible, the initial concentration is used. From the equilibrium constant, Gibbs adsorption free energy (ΔG_{ads}) is calculated using $\Delta G_{ads} = -RT \ln K_{ads}$. The fitting parameters, ΔG_{ads} and Γ_{max}, are shown in Table 1. The negative ΔG_{ads} values suggest that the adsorptions of these ECs at the air/aqueous interface are indeed favourable.

Within the uncertainty of the experimental measurements, the affinities of CBZ and β-ED for the air/aqueous interface are similar. This can be attributed to the fact that both molecules contain cyclic rings and are rigid; that is, they are likely to have similar driving forces for the surface. AMP exhibits a slightly diminished affinity compared to that of CBZ and β-ED. This can be attributed to the fact that AMP is positively charged, and thus more likely to be solvated. Within this set of compounds, the surface affinity trend appears to be the reverse of the solubility trend of these compounds. That is, the higher the solubility, the less surface active it is. Given that 4-PP is the most soluble of the

group, its affinity for the surface is also lower compared to the rest of the micropollutants studied. Many factors,[47] such as H-bonding with water, π–π interactions,[48] the influence of π–H bonding,[49] hydrophobic interactions[50] and entropic constraints, can dictate favourability, or the lack thereof, of these compounds for the water surface. What is clear is that these compounds do show proclivity for the air/water interface and elucidation of specific interactions is needed for further mechanistic insights.

It is worth noting that to determine the thermodynamic properties accurately, a broader concentration range of the micropollutants was chosen. Exploring this entire range, which exceeds the typical concentrations of these compounds detected in the aquatic environment, is necessary in order to observe the saturation in the isotherm data and thus obtain accurate fitting parameters. As noted above, the concentration of these compounds detected in the aquatic environment is generally in the nano to sub-micromolar range. Unless a large volume spill or a localized build-up occurs, the surface population of these contaminants will be small. Nevertheless, the equilibrium constant dictating the surface proclivity remains the same at all concentrations. Their propensity for the air/water interface is certain. More importantly, the adsorption free energy of these compounds for the hydrophobic air/water interface provides insights into the type of interactions these contaminants are likely to have with other surfaces. Our results show that a van der Waals type interaction or entropically driven adsorption process can provide a sufficient gradient for these small organic molecules to adsorb at the hydrophobic interfaces. That is, hydrophobic interactions can overcome the solvation energy observed for charged compounds (*e.g.*, AMP) and the H-bonding ability with water that all of these molecules exhibit. Thus, interaction of these compounds with particulate organic matter and microplastics, which often contain hydrophobic polymeric constituents, is expected.

Interaction with the lipid membrane

Next, we consider the effect of these micropollutants on the integrity of a zwitterionic phospholipid membrane. In the top panel of Fig. 2, the surface pressure *vs.* molecular area isotherms of DPPC in the absence and presence of a range of micropollutant concentrations are shown. As discussed in the Materials and methods section, the π–A isotherm is generated by compressing the insoluble lipid distributed on the water surface. The black solid trace in these graphs represents the isotherm of pure DPPC on the neat water surface. It displays various phases and phase transitions related to the conformational order as packing density increases (see Fig. 2A in ESI†).

Table 1 Air/aqueous adsorption thermodynamic parameters of micropollutants

|	AMP	CBZ	β-ED	4-PP
ΔG (kJ mol^{-1})	−30.9 ± 0.3	−32.3 ± 0.9	−33.2 ± 1.3	−27.8 ± 0.6
Γ_{max} (×10^{-6}) (mol m^{-2})	5.9 (±0.6)	0.9 ± 0.2	2.1 ± 0.9	6.8 ± 0.5
Area per molecule (Å^2 per molecule)	71 ± 3 at 120 μM	430 ± 150 at 70 μM	260 ± 36 at 37 μM	28.7 ± 0.2 at 4.3 mM
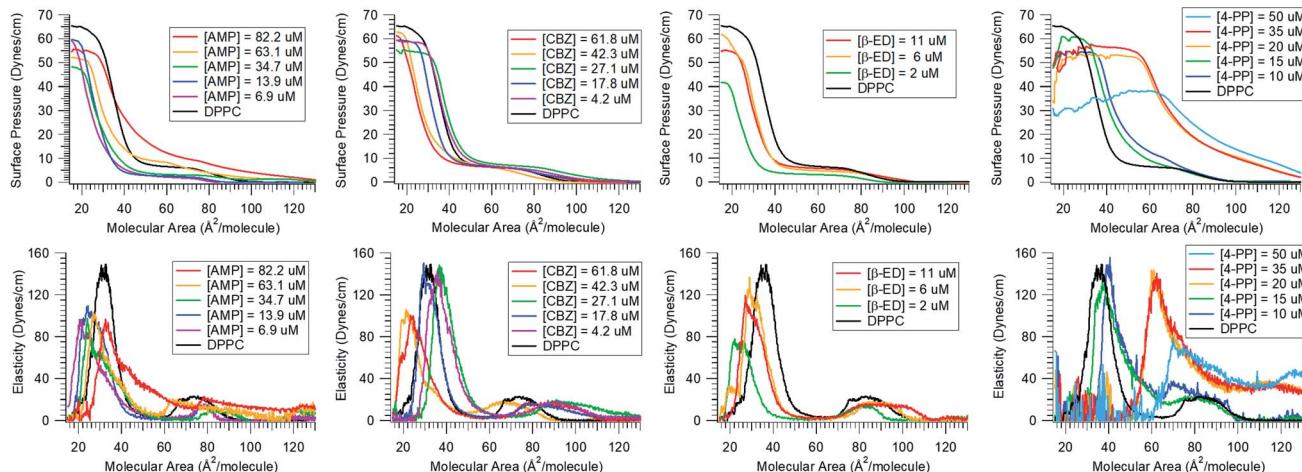
Fig. 2 Surface pressure *vs.* molecular area isotherms and elasticity *vs.* molecular area plots of DPPC in the presence of micropollutants, from left to right: AMP, CBZ, β-ED, and 4-PP. The concentration of the contaminant in the sub-phase is noted in the legend. The black trace is the measurement corresponding to DPPC in the absence of any micropollutant (*i.e.*, neat water sub-phase).

The common phases are gaseous (G), liquid-expanded (LE), and liquid-condensed (LC). If the subphase contains organic contaminants, they can interact with the lipid and thereby modify this phase behaviour. This would manifest in an altered $\pi-A$ isotherm showing changes in the surface pressure and shifts with respect to the molecular area. These variations map out the extent of interaction the molecule has with the lipid monolayer. Fig. 2 clearly shows that all the micropollutants investigated interact with the DPPC lipid membrane. This result is not surprising given the fact that these compounds show strong proclivity for the air/water interface.

A careful inspection of the isotherms reveal that the degree of the interactions varies with the identity of the micropollutant. For instance, in the presence of CBZ and β-ED, the surface pressure dropped (especially at low molecular area) for all concentrations and the isotherms shifted to the left relative to that of pure DPPC in neat water. The latter indicates that the mean molecular area is reduced in the presence of these compounds. This observation suggests that both CBZ and β-ED increase the condensation of lipid packing. Furthermore, it has been noted that the surface pressure at collapse is a measure of the lipid monolayer stability.[51] The lower the pressure at collapse, the less stable the monolayer. Thus, the lower surface pressure common to both CBZ and β-ED at all concentrations, suggests that these species have a destabilizing effect when a compact monolayer is formed. Another interesting feature to note is that the phases observed for pure DPPC are also observed in the presence of these species. The implication is that despite their interaction with DPPC, CBZ and β-ED do not drastically disrupt the DPPC phase behaviour.

This however is not the case when AMP or 4-PP are the micropollutants in the subphase. While in the low concentration range (6.9–34.7 μM) the behaviour is like that of CBZ and β-ED, at higher concentrations (63.1 μM and 82.2 μM), a clear shift to a higher surface pressure is observed for AMP at large molecular area where molecules are farther apart. At these concentrations the well-known phases of DPPC are appreciably altered. The LC phase is stretched over a larger area and the LC-LE transition is subdued. The most extensive changes in the DPPC isotherm are observed in the presence of 4-PP. Unlike the other micropollutants, 4-PP appears to increase the surface pressure. Even at the larger molecular area domain (gaseous phase), higher surface pressure is observed when the 4-PP concentration is at and above 20 μM. The presence of 4-PP leads to an expanded isotherm with a larger mean molecular area, which is indicative of a fluidizing effect, *i.e.*, disordering of DPPC.

One approach to understand the mechanical properties (*e.g.*, fluidity and rigidity) of the lipid membrane is through the concept of surface elasticity E,[5,44] defined as:

$$E = -A\left(\frac{\partial \pi}{\partial A}\right)_T \qquad (3)$$

Also known as the elastic modulus, in this equation, A is the total surface area and π is the surface pressure. This quantity represents a measure of the rigidity of the film; in other words, the film's resistance against compression. The larger the value of E, the greater the interaction between the lipid molecules. The bottom panel of Fig. 2 shows the plots of E against molecular area and the effect of various concentrations of the micropollutants. For neat DPPC, in the gaseous region (above 100 Å^2 per molecule), the surface elasticity is small due to the highly compressible and disordered insoluble monolayer. Two maxima are observed – the smallest representing the LE phase (a broad plateau in the range of $d \sim$65–90 Å^2 per molecule) and the larger corresponds to the LC phase (peak at $\sim$32 Å^2 per molecule).

Our results show that these micropollutants modify the elasticity of the DPPC monolayer. At all concentrations, both AMP and β-ED lower the elasticity of the LC phase, implying that DPPC is less rigid or ordered in the presence of these species.

Lowering of surface elasticity has also been attributed to partitioning of molecules into the lipid membrane and interaction with the hydrophobic tails.[52] Attractive interaction would explain a reduction in the molecular area facilitating a closely packed membrane. However, further investigations are necessary to elucidate this mechanism. For CBZ, a reduction in the LC phase elasticity is only seen at higher concentrations (42.3 μM and 61.8 μM). At lower CBZ concentrations, elasticity of the film is not significantly affected. In contrast, 4-PP has a substantial impact on the rigidity of the film. The interaction with this molecule appears to have increased the surface elasticity throughout the LC to G regions. At higher concentrations (35 μM and 50 μM), the shift in the peak position to a larger molecular area and an increase in elasticity also suggest that 4-PP makes the DPPC monolayer more fluid and hinders it from becoming compact. A plausible explanation for this is that 4-PP changes the tilt angle of the lipid to occupy a larger surface area.[53,54]

Another assessment we have performed is related to the favourability of the DPPC and micropollutant interaction. Since we are compressing the DPPC molecule in the absence and presence of a target compound, we can compare the Helmholtz free energy[44,45] (ΔF) of compression for these processes. Eqn (4) shows that ΔF is the integral (or area under the curve) of the $\pi-A$ isotherm.

$$\Delta F = \int_{A_1}^{A_2} \pi \, dA \tag{4}$$

For our calculation A_1 and A_2 were chosen to be 120 and 15 Å^2 per molecule, respectively. The relative (or the difference in) Helmholtz free energy of compression with (w) or without (w/o) micropollutants is thus:

$$\Delta\Delta F = \Delta F_{\text{w}} - \Delta F_{\text{w/o}} \tag{5}$$

Based on eqn (5), if $\Delta\Delta F$ is negative, less energy is required to compress the lipid in the presence of these compounds. This would imply either a favourable interaction of the ECs with the lipid molecules or a reduction of repulsive interaction between the DPPC molecules. Fig. 3 displays the effect of the micropollutants on $\Delta\Delta F$ as a function of their concentrations.

All three pharmaceuticals show a favourable interaction at low concentrations. As the AMP concentration increases, however, $\Delta\Delta F$ becomes less negative and exhibits a positive value at the highest concentration. It appears that at low concentrations, these compounds interact in a way that minimizes the net repulsive interaction between the lipid headgroups. AMP at higher concentrations, and thus higher surface population, acts to resist compression, leading to an increase in $\Delta\Delta F$. Interestingly, 4-PP leads to the most unfavourable interactions at all concentrations. 4-PP appears to occupy a significant surface area or cause the lipid molecules to orient flat such that the energy required to compress them is greater in its presence. Clearly, the organo-heterocyclic and the lipid like molecules show favourable interactions, whereas the benzenoid displays a hindrance effect.
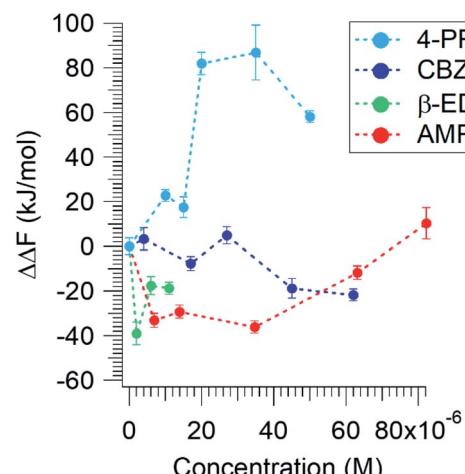
Fig. 3   The relative Helmholtz free energy of compression of DPPC as a function of concentration of different micropollutants.

Conclusions

In this communication we have demonstrated that amlodipine, carbamazepine, β-estradiol, and 4-propylphenol, all of which represent contaminants of emerging concern, show strong proclivity for the water surface. The extent of surface population and affinity vary for these compounds. The ΔG_{ads} trend, in the order of decreasing spontaneity of the physisorption process, is β-ED ∼ CBZ > AMP > 4-PP. It is also evident that both β-ED and CBZ occupy a larger surface area, whereas AMP and 4-PP can form a compact monolayer at their respective highest concentrations investigated. The air/water interface represents a hydrophobic environment. Natural water contains a plethora of surfaces including hydrophobic polymeric/aqueous interfaces. Thus, the finding suggests that these micropollutants will interact with these interfaces. Consideration of the interfacial interactions is thus important to accurately predict their fate and transport and determine their effectiveness in binding to various sorbents.

We have further studied the impact of these compounds on the mechanical properties and phase behaviour of a model lipid membrane. It is evident from the discussion that different classes of compounds have a distinct effect on DPPC monolayer formation. Overall, a similar effect on the DPPC phase behaviour is observed for both CBZ and β-ED. This can be attributed to the fact that these molecules are neutrally charged and structurally rigid (RBC = 0). In comparison, AMP shows a greater extent of interaction, especially at a higher concentration. The fact that AMP is positively charged, coulombic interaction between the zwitterionic headgroup of DPPC and AMP is thus likely responsible for the differences. Unlike the pharmaceutical ECs, 4-PP has a drastic impact on the structural integrity and phase behaviour of the DPPC monolayer. Both AMP and 4-PP have a greater degree of freedom with respect to bond rotation allowing numerous conformational possibilities of interaction with DPPC molecules.

This communication provides a preliminary insight into the surface activity of select classes of emerging organic pollutants. However, to extract additional fundamental properties, such as a correlation between the molecular structure and the type of surface interaction, more laboratory experiments are needed, and this is the focus of our ongoing research. For example, for deciphering the binding strength and how it varies with micropollutant functional groups, enthalpic and entropic contributions to ΔG_{ads} are necessary. To better elucidate the phase behaviour of biological membranes, specific chemical interactions and orientational analysis, as can be elucidated with various interfacial selective tools,[5,55,56] are warranted. At a fundamental level, these thermodynamic parameters can establish a structure–function relationship between various contaminants and surfaces. At a practical level, these interfacial parameters can help assess the fate and transport of these compounds or compounds belonging to a similar class. They can also be used to develop contaminant remediation methods based on adsorption techniques. Studies involving the detection and toxicity effect of emerging contaminants such as pharmaceuticals and personal care products are prominent. However, investigations pertinent to the interactions of these compounds with various soft interfaces, including biological membranes available in the aquatic environment, are limited. This study goes to show that organic ECs can exhibit proclivity for the air/water interface and have different disrupting effects on phospholipid membranes common in aquatic cells. Thus, this communication also highlights the need to better understand the interfacial properties of emerging contaminants.

Author contributions

Giada Dalla Pozza: Data curation, Formal analysis, Investigation, Methodology, Project administration, Validation; Danielle Deardorff: Data curation, Formal analysis, Investigation, Validation; Mahamud Subir: Conceptualization, Data curation, Formal Analysis, Funding acquisition, Investigation, Methodology, Project administration, Resources, Supervision, Visualization, Writing – original draft, Writing – review & editing.

Conflicts of interest

There are no conflicts to declare.

Acknowledgements

Notes and references

1 L. Chacón, L. Reyes, L. Rivera-Montero and K. Barrantes, in *Emerging Contaminants in the Environment*, ed. H. Sarma, D. C. Dominguez and W.-Y. Lee, Elsevier, 2022, pp. 111–136.

2 A. R. Datta, Q. Kang, B. Chen and X. Ye, in *Advances in Marine Biology*, ed. B. Chen, B. Zhang, Z. Zhu and K. Lee, Academic Press, 2018, vol. 81, pp. 97–128.

3 X. Tong, S. Mohapatra, J. Zhang, N. H. Tran, L. You, Y. He and K. Y.-H. Gin, *Water Res.*, 2022, **217**, 118418.

4 L. Kaylor, P. Skelly, M. Alsarrani and M. Subir, *Chemosphere*, 2022, **287**, 131953.

5 M. Subir and Y. Rao, *Environmental Interfacial Spectroscopy*, American Chemical Society, 2021, DOI: **10.1021/acsinfocus.7e5016**.

6 W. T. S. Cole, H. Wei, S. C. Nguyen, C. B. Harris, D. J. Miller and R. J. Saykally, *J. Phys. Chem. C*, 2019, **123**, 14362–14369.

7 V. M. Vulava, W. C. Cory, V. L. Murphey and C. Z. Ulmer, *Sci. Total Environ.*, 2016, **565**, 1063–1070.

8 S. Zhao, S. Xue, J. Zhang, Z. Zhang and J. Sun, *Sci. Rep.*, 2020, **10**, 3413.

9 H. Luo, C. Liu, D. He, J. Xu, J. Sun, J. Li and X. Pan, *J. Hazard. Mater.*, 2022, **423**, 126915.

10 T. Atugoda, M. Vithanage, H. Wijesekara, N. Bolan, A. K. Sarmah, M. S. Bank, S. You and Y. S. Ok, *Environ. Int.*, 2021, **149**, 106367.

11 S. Rizzuto, D. L. Baho, K. C. Jones, H. Zhang, E. Leu and L. Nizzetto, *Sci. Total Environ.*, 2021, **784**, 147208.

12 A. C. Sophia and E. C. Lima, *Ecotoxicol. Environ. Saf.*, 2018, **150**, 1–17.

13 B. S. Rathi and P. S. Kumar, *Environ. Pollut.*, 2021, **280**, 116995.

14 S. Alipoori, H. Rouhi, E. Linn, H. Stumpfl, H. Mokarizadeh, M. R. Esfahani, A. Koh, S. T. Weinman and E. K. Wujcik, *ACS Appl. Polym. Mater.*, 2021, **3**, 549–577.

15 E. K. Richmond, E. J. Rosi, D. M. Walters, J. Fick, S. K. Hamilton, T. Brodin, A. Sundelin and M. R. Grace, *Nat. Commun.*, 2018, **9**, 4491.

16 A. J. Ramirez, R. A. Brain, S. Usenko, M. A. Mottaleb, J. G. O'Donnell, L. L. Stahl, J. B. Wathen, B. D. Snyder, J. L. Pitt, P. Perez-Hurtado, L. L. Dobbins, B. W. Brooks and C. K. Chambliss, *Environ. Toxicol. Chem.*, 2009, **28**, 2587–2597.

17 C. Regnault, M. Usal, S. Veyrenc, K. Couturier, C. Batandier, A.-L. Bulteau, D. Lejon, A. Sapin, B. Combourieu, M. Chetiveaux, C. L. May, T. Lafond, M. Raveton and S. Reynaud, *Proc. Natl. Acad. Sci. U.S.A.*, 2018, **115**, E4416–E4425.

18 J. Oehlmann, U. Schulte-Oehlmann, W. Kloas, O. Jagnytsch, I. Lutz, K. O. Kusk, L. Wollenberger, E. M. Santos, G. C. Paull, K. J. W. Van Look and C. R. Tyler, *Philos. Trans. R. Soc. Lond. Ser. B Biol. Sci.*, 2009, **364**, 2047–2062.

19 A. Lajeunesse, G. Vernouillet, P. Eullaffroy, C. Gagnon, P. Juneau and S. Sauvé, *J. Environ. Monit.*, 2009, **11**, 723–725.

20 G. Vernouillet, P. Eullaffroy, A. Lajeunesse, C. Blaise, F. Gagné and P. Juneau, *Chemosphere*, 2010, **80**, 1062–1068.

21 E. Nazari and F. Suja, *Rev. Environ. Health*, 2016, **31**, 465–491.

22 H. Celle-Jeanton, D. Schemberg, N. Mohammed, F. Huneau, G. Bertrand, V. Lavastre and P. Le Coustumer, *Environ. Int.*, 2014, **73**, 10–21.

23 B. Björlenius, M. Ripszám, P. Haglund, R. H. Lindberg, M. Tysklind and J. Fick, *Sci. Total Environ.*, 2018, **633**, 1496–1509.

24 X. F. Zhou, C. M. Dai, Y. L. Zhang, R. Y. Surampalli and T. C. Zhang, *Environ. Monit. Assess.*, 2011, **173**, 45–53.

25 A. Jakimska, M. Śliwka-Kaszyńska, P. Nagórski, J. Namieśnik and A. Kot-Wasik, *PLoS One*, 2014, **9**, e109206.

26 Y. Xing, Y. Yu and Y. Men, *Environ. Sci. Water Res. Technol.*, 2018, **4**, 1412–1426.

27 S. Bhattacharya, P. Banerjee, P. Das, A. Bhowal, S. K. Majumder and P. Ghosh, *Sustain. Environ. Res.*, 2020, **30**, 17.

28 O. F. S. Khasawneh and P. Palaniandy, *Process Saf. Environ. Prot.*, 2021, **150**, 532–556.

29 M. Suzumura, *Talanta*, 2005, **66**, 422–434.

30 C. Parzanini, C. C. Parrish, J.-F. Hamel and A. Mercier, *PLoS One*, 2018, **13**, e0207395.

31 C. C. Parrish, *ISRN Oceanography*, 2013, **2013**, 604045.

32 L. Farine, M. Niemann, A. Schneider and P. Bütikofer, *Sci. Rep.*, 2015, **5**, 16787.

33 M. Zhong, T. Wang, W. Zhao, J. Huang, B. Wang, L. Blaney, Q. Bu and G. Yu, *Engineering*, 2022, **11**, 111–125.

34 C. J. Carter and R. A. Blizard, *Neurochem. Int.*, 2016, **101**, 83–109.

35 D. J. Lapworth, N. Baran, M. E. Stuart and R. S. Ward, *Environ. Pollut.*, 2012, **163**, 287–303.

36 M. Patel, R. Kumar, K. Kishor, T. Mlsna, C. U. Pittman and D. Mohan, *Chem. Rev.*, 2019, **119**, 3510–3673.

37 P. Dotan, A. Tal and S. Arnon, *Sci. Total Environ.*, 2017, **575**, 588–594.

38 A. Priac, N. Morin-Crini, C. Druart, S. Gavoille, C. Bradu, C. Lagarrigue, G. Torri, P. Winterton and G. Crini, *Arab. J. Chem.*, 2017, **10**, S3749–S3773.

39 M. Solé, M. J. López de Alda, M. Castillo, C. Porte, K. Ladegaard-Pedersen and D. Barceló, *Environ. Sci. Technol.*, 2000, **34**, 5076–5083.

40 D. S. Wishart, Y. D. Feunang, A. C. Guo, E. J. Lo, A. Marcu, J. R. Grant, T. Sajed, D. Johnson, C. Li, Z. Sayeeda, N. Assempour, I. Iynkkaran, Y. Liu, A. Maciejewski, N. Gale, A. Wilson, L. Chin, R. Cummings, D. Le, A. Pon, C. Knox and M. Wilson, *Nucleic Acids Res.*, 2017, **46**, D1074–D1082.

41 D. S. Wishart, A. Guo, E. Oler, F. Wang, A. Anjum, H. Peters, R. Dizon, Z. Sayeeda, S. Tian, B. L. Lee, M. Berjanskii, R. Mah, M. Yamamoto, J. Jovel, C. Torres-Calzada, M. Hiebert-Giesbrecht, V. W. Lui, D. Varshavi, D. Varshavi, D. Allen, D. Arndt, N. Khetarpal, A. Sivakumaran, K. Harford, S. Sanford, K. Yee, X. Cao, Z. Budinski, J. Liigand, L. Zhang, J. Zheng, R. Mandal, N. Karu, M. Dambrova, H. B. Schiöth, R. Greiner and V. Gautam, *Nucleic Acids Res.*, 2022, **50**, D622–d631.

42 T. Williams, C. Walsh, K. Murray and M. Subir, *Environ. Sci.: Processes Impacts*, 2020, **22**, 1190–1200.

43 K. M. Lewis and R. D. Archer, *Steroids*, 1979, **34**, 485–499.

44 H.-J. Butt, K. Graf and M. Kappl, *Physics and Chemistry of Interfaces*, Wiley-VCH Verlag GmbH & Co. KGaA, Weinhem, 2003.

45 A. W. A. a. A. P. Gast, *Physical Chemistry of Surfaces*, John-Wiley & Sons, Inc., 1997.

46 I. Mukherjee, S. P. Moulik and A. K. Rakshit, *J. Colloid Interface Sci.*, 2013, **394**, 329–336.

47 C. T. Chiou, in *Partition and Adsorption of Organic Contaminants in Environmental Systems*, pp. 1–13, 2002, DOI: 10.1002/0471264326.ch1.

48 D. Quiñonero, A. Frontera, C. Garau, P. Ballester, A. Costa and P. M. Deyà, *ChemPhysChem*, 2006, **7**, 2487–2491.

49 S. Enami, T. Fujii, Y. Sakamoto, T. Hama and Y. Kajii, *J. Phys. Chem.*, 2016, **120**, 9224–9234.

50 P. Setny, R. Baron and J. A. McCammon, *J. Chem. Theory Comput.*, 2010, **6**, 2866–2871.

51 A. Wnętrzak, K. Łątka and P. Dynarowicz-Łątka, *J. Membr. Biol.*, 2013, **246**, 453–466.

52 V. P. N. Geraldo, F. J. Pavinatto, T. M. Nobre, L. Caseli and O. N. Oliveira, *Chem. Phys. Lett.*, 2013, **559**, 99–106.

53 G. Ma and H. C. Allen, *Photochem. Photobiol.*, 2006, **82**, 1517–1529.

54 A. Bañuelos-Frias, V. M. Castañeda-Montiel, E. R. Alvizo-Paez, E. A. Vazquez-Martinez, E. Gomez and J. Ruiz-Garcia, *Front. Phys.*, 2021, **9**, 636149.

55 F. Wei, W. Xiong, W. Li, W. Lu, H. C. Allen and W. Zheng, *Phys. Chem. Chem. Phys.*, 2015, **17**, 25114–25122.

56 L. Fu, Z. Wang, V. S. Batista and E. C. Y. Yan, *J. Diabetes Res.*, 2016, **2016**, 7293063s.

© 2022 The Author(s). Published by the Royal Society of Chemistry

Environ. Sci.: Adv., 2022, **1**, 430–437 | **437**